Transport Coefficients in Yang-Mills Theory and QCD

Nicolai Christiansen,[1] Michael Haas,[1] Jan M. Pawlowski,[1,2] and Nils Strodthoff[1]
[1]Institut für Theoretische Physik, Universität Heidelberg, Philosophenweg 16, 69120 Heidelberg, Germany
[2]ExtreMe Matter Institute EMMI, GSI Helmholtzzentrum für Schwerionenforschung mbH, Planckstrasse 1, 64291 Darmstadt, Germany

(Received 23 January 2015; revised manuscript received 24 June 2015; published 10 September 2015)

We calculate the shear-viscosity-over-entropy-density ratio η/s in Yang-Mills theory from the Kubo formula using an exact diagrammatic representation in terms of full propagators and vertices using gluon spectral functions as external input. We provide an analytic fit formula for the temperature dependence of η/s over the whole temperature range from a glueball resonance gas at low temperatures, to a high-temperature regime consistent with perturbative results. Subsequently, we provide a first estimate for η/s in QCD.

DOI: 10.1103/PhysRevLett.115.112002 PACS numbers: 12.38.Aw, 11.15.Tk

Introduction.—The experimental heavy-ion programs at the RHIC [1,2] and at the LHC [3] explore the physics of the quark-gluon plasma (QGP). It turns out that the dynamics of the hot plasma created in heavy-ion collisions is well described by hydrodynamics. Therefore, the determination of transport coefficients in the QGP is of great interest. One aspect is that the inference of the initial-state physics requires a precise description of the hydrodynamical evolution, which, in turn, depends on transport coefficients as microscopic input [4]. In particular, the viscosity-over-entropy ratio η/s governs the efficiency of the conversion of the initial spatial anisotropy into a momentum anisotropy of the final state.

For the determination of η/s and its temperature dependence in the quark-gluon plasma, theoretical approaches face several challenges. The temperature regimes below and above the critical temperature T_c are characterized by different degrees of freedom, and for temperatures $T \lesssim 2T_c$, nonperturbative effects become important. Of particular interest is the vicinity of T_c, where the minimum for η/s is expected [5,6]. A universal lower bound for η/s of $1/4\pi$ was conjectured in Ref. [7] using the AdS/CFT correspondence. Indeed, measurements of the elliptic flow v_2 indicate a value for η/s which is of the order of this lower bound [8]. The bound has been tested theoretically with several methods for the QGP [9–15] but also for other potentially perfect liquids, such as ultracold atoms [16–18].

The Kubo formulas relate η to the energy-momentum tensor (EMT). Spectral functions are real-time quantities and cannot be obtained directly from Euclidean correlation functions. However, the direct calculation of real-time correlation functions represents a notoriously difficult problem in nonperturbative approaches to quantum field theory. Even though first computations in this direction have been performed, e.g., in Refs. [19,20], we shall utilize Euclidean correlation functions within a numerical analytic continuation.

In this Letter, we study the shear-viscosity-over-entropy ratio η/s in pure $SU(3)$ Landau gauge Yang-Mills (YM) theory within the approach setup in Ref. [9]. In the present work, we considerably generalize the approach, also aiming at quantitative precision. We apply an exact functional relation that allows a representation of the EMT correlation function in terms of full propagators and vertices of the gluon field. The analysis covers the entire temperature range from the glueball regime below the critical temperature T_c, up to the ultraviolet where perturbation theory is applicable. In particular, this resolves the nonperturbative domain at temperatures $T \lesssim 2T_c$. We provide a global, analytic fit formula for η/s which extends the well-known perturbative high-temperature behavior to the nonperturbative temperature regime. Based on this description for pure gauge theory, a first estimate for η/s in full QCD is derived.

YM shear viscosity from gluon spectral functions.—The shear viscosity is related to the spectral function $\rho_{\pi\pi}$ of the spatial traceless part π_{ij} of the energy-momentum tensor via the Kubo relation

$$\eta = \lim_{\omega\to 0} \frac{1}{20} \frac{\rho_{\pi\pi}(\omega, \vec{0})}{\omega}, \tag{1}$$

where

$$\rho_{\pi\pi}(\omega, \vec{p}) = \int \frac{d^4x}{(2\pi)^4} e^{-i\omega x_0 + i\vec{p}\,\vec{x}} \langle [\pi_{ij}(x), \pi_{ij}(0)] \rangle. \tag{2}$$

For the computation of Eq. (2), we use the fact that a general correlation function of composite operators can be expanded in terms of full propagators and full vertices of the elementary fields [9,21],

$$\langle \pi_{ij}[\hat{A}] \pi_{ij}[\hat{A}] \rangle = \pi_{ij} \left[G_{A\phi_k} \frac{\delta}{\delta \phi_k} + A \right] \pi_{ij} \left[G_{A\phi_k} \frac{\delta}{\delta \phi_k} + A \right], \tag{3}$$

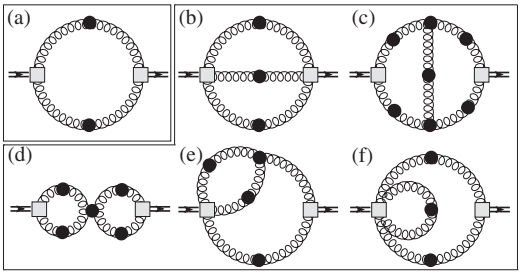

FIG. 1. Types of diagrams contributing to the correlation function of the energy-momentum tensor up to two-loop order: one-loop (a), sunset (b), Maki-Thompson (c), eight (d), squint (e), one-loop with vertex correction (f). Squares denote vertices derived from the EMT; all propagators and vertices are fully dressed.

where $\phi = (A, c, \bar{c})$ denotes the expectation value of the fluctuation (super)field $\hat{\phi}$, e.g., $A = \langle \hat{A} \rangle$, and $G_{\phi_i \phi_j} = \langle \hat{\phi}_i \hat{\phi}_j \rangle - \langle \hat{\phi}_i \rangle \langle \hat{\phi}_j \rangle$ denotes the propagator of the respective fields. This yields a diagrammatic representation in terms of a finite number of diagrams involving full propagators and vertices; see Fig. 1 for the types of diagrams appearing in the full expansion up to two-loop order. We emphasize that Eq. (3) is an exact relation whose finite diagrammatics should not be confused with a perturbative expansion in an infinite series of Feynman diagrams. The internal vertices arise from functional derivatives of the full propagator in Eq. (3) and are, therefore, automatically fully dressed. However, the RG invariance of the left-hand side of Eq. (3) only carries over to the right-hand side if also the external vertices derived from the EMT are dressed with appropriate wave-function renormalization factors and running couplings. This argument is supported by the flow equation for the EMT itself, which can be derived from the flow equation for composite operators [21], where full vertices are generated during the flow. More heuristically, this can also be seen in a skeleton expansion. Therefore, Eq. (2) generates diagrams up to loop order six, but these can be recast as diagrams of maximal order three with dressed external vertices.

The natural framework for such a calculation is the real-time formalism based on the Schwinger-Keldysh closed time path. Within such a setup, one never has to resort to Euclidean field theory. Here one distinguishes two branches of the time contour, conventionally denoted by $+/-$ along with separate fields and sources. Correlation functions, thus, become matrix valued. In thermal equilibrium, the propagator iG can be parametrized solely in terms of the spectral function $\rho(\omega, \vec{p})$ according to (cf. Ref. [22] for the free case)

$$\begin{aligned} G^{\pm\pm}(\omega, \vec{p}) &= \pm \mathrm{PV} \int_{-\infty}^{\infty} d\bar{\omega} \frac{\rho(\bar{\omega}, \vec{p})}{\omega - \bar{\omega}} - i\left(n(\omega) + \frac{1}{2}\right)\rho(\omega, \vec{p}), \\ G^{+-}(\omega, \vec{p}) &= -in(\omega)\rho(\omega, \vec{p}), \\ G^{-+}(\omega, \vec{p}) &= -i\big(n(\omega) + 1\big)\rho(\omega, \vec{p}), \end{aligned} \tag{4}$$

where $n(\omega) = 1/[\exp(\omega/T) + 1]$ denotes the Bose distribution function. The spectral function is defined as

$$\rho(\omega, \vec{p}) = i\big(G^{-+}(\omega, \vec{p}) - G^{+-}(\omega, \vec{p})\big). \tag{5}$$

Using the Kubo-Martin-Schwinger (KMS) condition for the propagators, we find for the spectral function of the energy-momentum tensor

$$\rho_{\pi\pi}(\omega, \vec{p}) = i(1 - e^{-\beta\omega}) G^{-+}_{\pi\pi}(\omega, \vec{p}). \tag{6}$$

Inserting Eq. (6) into Eq. (1) implies

$$\eta = i \frac{\beta}{20} G^{-+}_{\pi\pi}(0, 0). \tag{7}$$

In this Letter, we present the full two-loop diagrammatics. There are five types of two-loop diagrams arising from Eq. (3); see Fig. 1. The branch indices of the external vertices are fixed by Eq. (7) as $-+$, whereas we sum over internal branch indices. Thus, unlike in the one-loop case, at two-loop level, the principal value parts of propagators with equal branch indices can occur. However, at two-loop level, possibly UV-divergent contributions cancel due to a left-right symmetry after combining the appropriate diagrams. This is no longer true beyond two loop, where diagrams with divergent subdiagrams arise.

The only nontrivial input in our calculation, apart from the running coupling α_s, is the gluon spectral function obtained using the maximum entropy method (MEM) with Euclidean functional renormalization group (FRG) data as input. For details about MEM and gluon spectral functions, we refer the reader to Ref. [9]. Using data from Ref. [23], the running coupling $\alpha_s(q, T)$ is calculated as

$$\alpha_s(q, T) = \frac{z^2_{\bar{c}Ac}(q, T)}{4\pi Z_T(q, T) Z_c(q, T)^2}, \tag{8}$$

with the dressing functions $z_{\bar{c}Ac}, Z_c, Z_T$ of the ghost-gluon vertex, the ghost propagator, and the transverse gluon propagator. All couplings that appear in the vertices are fully dressed running couplings. Here we use the ghost-gluon coupling from above for all vertices consistent with Slavnov-Taylor identities for $p \gtrsim 2$ GeV [24]. We use classical tensor structures for internal and external vertices. Other tensor structures are negligible in this regime; see Refs. [24,25]. For each two-loop diagram, we integrate out one loop momentum. Considering the remaining loop momentum, all integrands are peaked in the vicinity of some value $(q_{0,\max}, \vec{q}_{\max})$. This leads to $q_{\max}(T) = \sqrt{q^2_{0,\max} + \vec{q}^2_{\max}} \approx 7T$ where the running couplings $\alpha_s(q, T)$ are evaluated in order to minimize the impact of the neglected momentum dependence of the vertices. This defines a temperature-dependent vertex coupling $\alpha_{s,\mathrm{vert}}(T) = \alpha_s(7T, T)$.

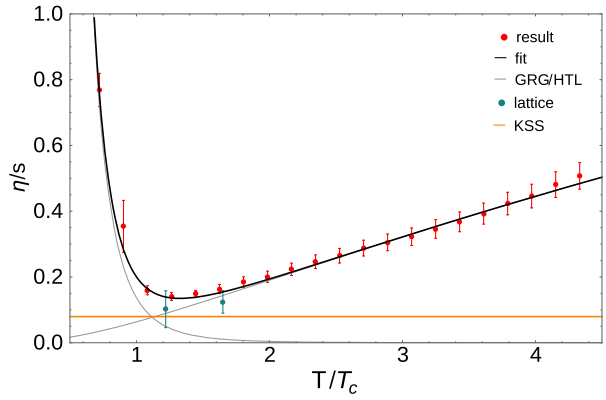

FIG. 2 (color online). Full Yang-Mills result (red) for η/s in comparison to lattice results [12,13] (blue) and the AdS/CFT bound of Kovtun, Son and Starinets (KSS) (orange). In addition, the plot shows the analytic fit given in Eq. (11) and its two components. The ratio η/s shows a minimum at $T_{\min} \approx 1.26 T_c$ with a value of 0.14.

Results.—Figure 2 shows the full two-loop result for η/s employing the lattice entropy density from Ref. [26] including all diagrams from Fig. 1. The data show, as expected on general grounds, a clear minimum at $T_{\min} \approx 1.26 T_c$. The minimal value $\eta/s(T_{\min}) = 0.14$ is well above the AdS/CFT bound, where the error bars represent the combined systematic errors from MEM and the FRG calculation. The lattice data [12,13] are in good agreement with our results, supporting the reliability of both methods. The inset in Fig. 3 shows the comparison to the one-loop calculation [9], illustrating the very good agreement around T_c. This confirms the argument concerning the optimization of the RG scheme around T_c [9]. Only at larger temperatures, the data points of the one-loop calculation lie outside the error bars of the full result. For large temperatures, the dominant two-loop contributions arise from the Maki-Thompson and the eight (see Fig. 3)

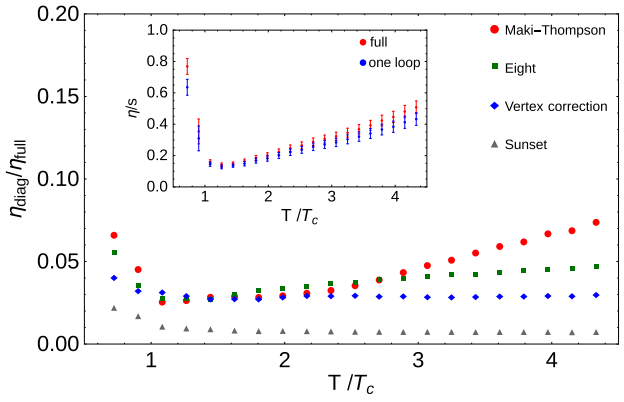

FIG. 3 (color online). Relative contributions from different diagram types to the two-loop viscosity as a function of temperature. The squint contribution is orders of magnitude smaller and not shown. The inset shows the comparison to the one-loop result [9].

that resum classes of ladder diagrams. This is consistent with the conventional picture in perturbative expansions where ladder resummations are required to obtain the correct result for the viscosity [27,28]. Note that diagrams with overlapping loops are potentially suppressed as the spectral functions are peaked in a narrow region in momentum space. Because of the additional phase space suppression, we expect that diagrams with more than two loops are negligible. We have checked this suppression in a first assessment of three-loop diagrams.

We provide a global fit function for $\eta/s(T)$, which emphasizes the physical picture underlying the temperature behavior and is well suited for phenomenological applications. This parametrization has to cover temperature ranges corresponding to vastly different physical situations. At large temperatures $T \gg T_c$, the degrees of freedom are gluons which can eventually be treated perturbatively. By contrast, at small temperatures $T \lesssim T_c$, YM theory can effectively be described as a glueball resonance gas (GRG). Finally, there is a transition region between these two asymptotic regimes whose description requires nonperturbative techniques.

In the high-temperature regime, perturbation theory is applicable, and η/s is given as a function of the strong coupling α_s only. It turns out that the hard-thermal loop (HTL) resummed data [29] are well described by the functional form

$$\frac{\eta}{s}(\alpha_s) = \frac{a}{\alpha_s^{\gamma}}, \tag{9}$$

with a coefficient a and a scaling exponent $\gamma = 1.6(1)$. We aim to extract a nonperturbative extension of the above parametrization based on our data. In the region $T_c - 3T_c$, strong correlations become important and perturbation theory breaks down. This raises the question of a suitable running coupling, as there is no unique definition of α_s beyond two loop. A quasiparticle picture suggests that an appropriate choice of α_s can be deduced from a heavy quark potential [30,31].

An analytic expression for a coupling that generates a linearly rising static quark potential at large distances is given by [32–34]

$$\alpha_{s,\mathrm{HQ}}(z) = \frac{1}{\beta_0}\frac{z^2-1}{z^2 \log z^2}, \tag{10}$$

where z denotes a dimensionless momentum variable. At large momenta, it approaches the one-loop running coupling, where $\beta_0 = 33/(12\pi)$ denotes the coefficient in the one-loop beta function of pure $SU(3)$ Yang-Mills theory. The scale identification is implemented by regarding $\alpha_{s,\mathrm{HQ}}$ as a function of $z = cT/T_c$ with a scale identification factor c. By construction, the divergence of Eq. (10) at zero momentum leads to a vanishing contribution of Eq. (9) to η/s at zero temperature. As an estimate for a lower bound for a reasonable high-temperature fit, we consider the trace anomaly as a hint from QCD thermodynamics, which starts

to develop a T^4 behavior for $T \gtrsim 2T_c$ [35]. Using $T > 3T_c$ as a conservative estimate, our data are well described by the scaling form (9) with the running coupling (10) and parameters $a = 0.15$ and $c = 0.66$. One should note that whereas the heavy quark potential coupling takes a rather large value $\alpha_{s,\mathrm{HQ}}(cT/T_c)|_{T=T_c} \approx 1.77$ at T_c, the vertex coupling $\alpha_{s,\mathrm{vert}}(T_c) \approx 0.76$ corresponding to a value of $\alpha_{s,\mathrm{vert}}^{\overline{\mathrm{MS}}}(T_c) \approx 0.35$ after conversion to the $\overline{\mathrm{MS}}$ scheme [36] is comparably small. This supports the validity of resummation arguments at moderately large temperatures but also underlines the nonuniqueness of the definition of a running coupling in the nonperturbative regime around T_c. The fit (9) can be extended to even lower temperatures $T \gtrsim 1.8T_c$, where it is still in very good agreement with our data; see Fig. 2. These findings hint at the validity of a quasiparticle picture even at considerably low temperatures.

Below T_c, the effective degrees of freedom change from gluons to glueballs. The latter are automatically included in the present setup [37]. For a gas of heavy particles with $m \gg T$, the viscosity-over-entropy ratio scales as $\exp(m/T)$. Indeed, the low-temperature regime of our data is well described by such an exponential. However, due to the small number of data points and the comparably large error bars below T_c, no precise statements about this regime are possible. We aim to describe, in particular, the mid-temperature regime by a simple global fit function. A power law for small temperatures takes into account the dissociation of glueballs above T_c and is equally consistent with our data for $T \lessapprox T_c$. This is superposed with the high-temperature asymptotics using an exponent $\gamma = 1.6$ determined from Eq. (9). This leads to a global parametrization of the form

$$\frac{\eta}{s}(T) = \frac{a}{\alpha_{s,HQ}^{\gamma}(cT/T_c)} + b\left(\frac{T}{T_c}\right)^{-\delta}. \tag{11}$$

With $a = 0.15(2)$, $b = 0.14(1)$, $c = 0.66(6)$, $\delta = 5.1(1)$, and $\gamma = 1.6(1)$ as given above, this fit describes our data very well; see Fig. 2.

The analytic fit function (11) for η/s in YM theory enables us to provide a first estimate of η/s in full QCD, again based on the idea of superposing a low- and high-temperature behavior term. The procedure consists of three separate steps. First, one has to take into account the difference in scales and the running couplings in YM and QCD. This involves replacing the coefficient β_0 in Eq. (10) by its QCD value, $\beta_{0,\mathrm{QCD}} = (33 - 2N_f)/(12\pi)$. Additionally, one has to set a scale by fixing the ratio of the running couplings in YM and QCD at a certain point. In our setup, the characteristic scale is the critical temperature T_c. For the phase transition to the confinement phase to take place, the strong coupling usually needs to exceed a certain critical value $\alpha_s(T) = \alpha_{\mathrm{crit}}$. On general grounds, one can argue that the critical values in YM theory and QCD are of comparable size. This argument is supported by the fact

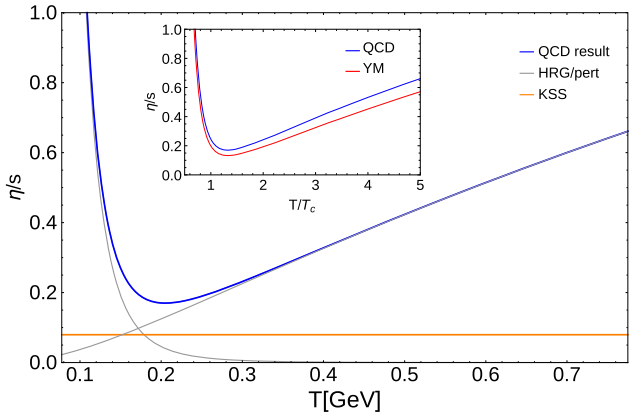

FIG. 4 (color online). Estimate for η/s in QCD which shows a minimum at $T_{\mathrm{min}} \approx 1.3T_c$ at a value of 0.17. The inset shows the comparison to the YM results for temperatures normalized by the respective critical temperatures.

that the values of α_{crit} for the vertex couplings tend to coincide. Consequently, we impose the condition

$$\alpha_{s,\mathrm{HQ}}^{N_f=0}(cT/T_c)|_{T=T_c} = \alpha_{s,\mathrm{HQ}}^{N_f=3}(c_{\mathrm{QCD}}T/T_c)|_{T=T_c}. \tag{12}$$

This fixes the scale factor as $c_{\mathrm{QCD}} = 0.79$. Second, one has to take into account genuine quark contributions that are not encoded in the change of the running couplings. Denoting the quark contributions to viscosity and entropy as $\Delta\eta$ and Δs, respectively, we write

$$\left.\frac{\eta}{s}\right|_{\mathrm{QCD}} = \frac{\eta_{\mathrm{YM}} + \Delta\eta}{s_{\mathrm{YM}} + \Delta s} = \left.\frac{\eta}{s}\right|_{\mathrm{YM},\alpha_s^{\mathrm{YM}} \to \alpha_s^{\mathrm{QCD}}} \left(\frac{1 + \frac{\Delta\eta}{\eta_{\mathrm{YM}}}}{1 + \frac{\Delta s}{s_{\mathrm{YM}}}}\right), \tag{13}$$

and estimate the ratios $\Delta\eta/\eta_{\mathrm{YM}}$ and $\Delta s/s_{\mathrm{YM}}$ using leading-order perturbative results. For $N_f = 3$, we find $\Delta\eta/\eta_{\mathrm{YM}} \approx 2.9$ [38,39] and $\Delta s/s_{\mathrm{YM}} \approx \frac{21}{32}N_f \approx 2.0$ [40,41], leading to an overall correction factor of approximately $4/3$. Finally, in the low-temperature regime, one has to replace the pure glueball resonance gas by a hadron resonance gas (HRG).

In summary, the final estimate for QCD takes the form (11) but with the following QCD parameters replacing the corresponding YM values: $a_{\mathrm{QCD}} \approx 4/3a$, $b_{\mathrm{QCD}} = 0.16(1)$, $\delta_{\mathrm{QCD}} = 5$, where b_{QCD} results from a fit to the data from Ref. [42]. Additionally, the full QCD $\alpha_{s,\mathrm{HQ}}^{Nf=3}(c_{\mathrm{QCD}}T/T_c)$ with $c_{\mathrm{QCD}} = 0.79$ replaces the pure-glue beta function, whereas the perturbative exponent $\gamma = 1.6$ remains unchanged.

This procedure yields the final result shown in Fig. 4. Plotted in terms of temperatures normalized by the respective critical temperatures, the QCD curve is shifted slightly upwards compared to the YM result; see the inset of Fig. 4. The shape resembles that of the YM result with a minimum value of 0.17 at $T_{\mathrm{min}} \approx 1.3T_c$.

Summary and conclusions.—We have computed η/s in pure YM theory over a large temperature range. The setup is based on an exact functional relation for the spectral function of the energy-momentum tensor involving full gluon propagators and vertices. The only inputs are the gluon spectral function and the running coupling α_s extracted from Euclidean FRG data [23]. As a highly nontrivial result, the global temperature behavior of η/s can be described as a direct sum of a glueball resonance gas contribution with an algebraic decay at small temperatures and a high-temperature contribution consistent with HTL resummed perturbation theory. Finally, we have provided a first estimate for η/s in QCD.

The authors thank L. McLerran, G. Denicol, H. Niemi, and D. Rischke for discussions. This work is supported by the Helmholtz Alliance HA216/EMMI and the Grant No. ERC-AdG-290623. N. C. acknowledges funding from the Heidelberg Graduate School of Fundamental Physics.

[1] K. Adcox *et al.* (PHENIX Collaboration), Nucl. Phys. **A757**, 184 (2005).
[2] J. Adams *et al.* (STAR Collaboration), Nucl. Phys. **A757**, 102 (2005).
[3] K. Aamodt *et al.* (ALICE Collaboration), Phys. Rev. Lett. **105**, 252302 (2010).
[4] H. Niemi, G. S. Denicol, P. Huovinen, E. Molnar, and D. H. Rischke, Phys. Rev. Lett. **106**, 212302 (2011).
[5] L. P. Csernai, J. I. Kapusta, and L. D. McLerran, Phys. Rev. Lett. **97**, 152303 (2006).
[6] T. Hirano and M. Gyulassy, Nucl. Phys. **A769**, 71 (2006).
[7] P. K. Kovtun, D. T. Son, and A. O. Starinets, Phys. Rev. Lett. **94**, 111601 (2005).
[8] U. Heinz and R. Snellings, Annu. Rev. Nucl. Part. Sci. **63**, 123 (2013).
[9] M. Haas, L. Fister, and J. M. Pawlowski, Phys. Rev. D **90**, 091501 (2014).
[10] G. Aarts and J. M. Martinez Resco, J. High Energy Phys. 04 (2002) 053.
[11] Z. Xu and C. Greiner, Phys. Rev. Lett. **100**, 172301 (2008).
[12] H. B. Meyer, Phys. Rev. D **76**, 101701 (2007).
[13] H. B. Meyer, Nucl. Phys. **A830**, 641c (2009).
[14] R. Lang and W. Weise, Eur. Phys. J. A **50**, 63 (2014).
[15] R. Marty, E. Bratkovskaya, W. Cassing, J. Aichelin, and H. Berrehrah, Phys. Rev. C **88**, 045204 (2013).
[16] B. A. Gelman, E. V. Shuryak, and I. Zahed, Phys. Rev. A **72**, 043601 (2005).
[17] J. E. Thomas, Nucl. Phys. **A830**, 665c (2009).
[18] T. Schaefer, Annu. Rev. Nucl. Part. Sci. **64**, 125 (2014).
[19] K. Kamikado, N. Strodthoff, L. von Smekal, and J. Wambach, Eur. Phys. J. C **74**, 2806 (2014).
[20] S. Strauss, C. S. Fischer, and C. Kellermann, Phys. Rev. Lett. **109**, 252001 (2012).
[21] J. M. Pawlowski, Ann. Phys. (Amsterdam) **322**, 2831 (2007).
[22] A. K. Das, *Finite Temperature Field Theory* (World Scientific, Singapore, 1997).
[23] L. Fister and J. M. Pawlowski, arXiv:1112.5440.
[24] M. Mitter, J. M. Pawlowski, and N. Strodthoff, Phys. Rev. D **91**, 054035 (2015).
[25] G. Eichmann, R. Williams, R. Alkofer, and M. Vujinovic, Phys. Rev. D **89**, 105014 (2014).
[26] S. Borsanyi, G. Endrodi, Z. Fodor, S. Katz, and K. Szabo, J. High Energy Phys. 07 (2012) 056.
[27] S. Jeon, Phys. Rev. D **52**, 3591 (1995).
[28] S. Jeon and L. G. Yaffe, Phys. Rev. D **53**, 5799 (1996).
[29] P. B. Arnold, G. D. Moore, and L. G. Yaffe, J. High Energy Phys. 05 (2003) 051.
[30] J. L. Richardson, Phys. Lett. **82B**, 272 (1979).
[31] F. Karbstein, A. Peters, and M. Wagner, J. High Energy Phys. 09 (2014) 114.
[32] A. V. Nesterenko, Phys. Rev. D **62**, 094028 (2000).
[33] A. Nesterenko, Int. J. Mod. Phys. A **18**, 5475 (2003).
[34] F. Schrempp, J. Phys. G **28**, 915 (2002).
[35] J. O. Andersen, L. E. Leganger, M. Strickland, and N. Su, Phys. Rev. D **84**, 087703 (2011).
[36] L. von Smekal, K. Maltman, and A. Sternbeck, Phys. Lett. B **681**, 336 (2009).
[37] M. Haas, A. Maas, and J. M. Pawlowski (to be published).
[38] J.-W. Chen, Y.-F. Liu, Y.-K. Song, and Q. Wang, Phys. Rev. D **87**, 036002 (2013).
[39] P. B. Arnold, G. D. Moore, and L. G. Yaffe, J. High Energy Phys. 11 (2000) 001.
[40] P. B. Arnold and C.-x. Zhai, Phys. Rev. D **51**, 1906 (1995).
[41] J. O. Andersen, E. Braaten, and M. Strickland, Phys. Rev. D **61**, 074016 (2000).
[42] N. Demir and S. A. Bass, Phys. Rev. Lett. **102**, 172302 (2009).